Sara Caracol Gomes – Institute for Bioengineering and Biosciences, Instituto Superior Técnico

Supervisor – Doctor Leonilde de Fátima Morais Moreira

Genetic and environmental conditions influencing cellular aggregates formation in *Burkholderia multivorans*

Abstract: Chronic respiratory bacterial infections are a significant healthcare cost. One such case is the respiratory infections of cystic fibrosis patients, often caused by opportunistic pathogens of the *Burkholderia cepacia* complex, which are associated with increasing morbidity and mortality. Bacterial transitions to chronicity are characterized by phenotypic changes, thought to reflect adaptation to stresses of the CF lung. Yet, how these stressors act on bacteria to drive the transition to chronic infection is unknown. We hypothesize that stressors act on cells and trigger the formation of cellular aggregates. To test this hypothesis, we analysed and confirmed that the majority of the *B. multivorans* isolates recovered from 9 patients do form cell aggregates and this number increases in a medium mimicking the CF lung. Sub-inhibitory concentrations of ciprofloxacin were the best trigger of aggregates formation. Regarding putative molecular players in aggregates formation, it was confirmed the role of lactate dehydrogenase in this process. With the aim of finding additional genes involved in cellular aggregation, an evolution experiment was performed. Not only it was possible to evolve this phenotype under laboratory settings, but by sequencing the whole genome of an evolved colony, we identified genes involved in pili synthesis and peptidoglycan degradation as possible involved in the formation of this multicellular structures.

Introduction

Cystic Fibrosis (CF) patients suffer from permanent polymicrobial lung infections caused by several types of bacteria, including *Pseudomonas aeruginosa* and *Burkholderia cepacia* complex (Bcc) bacteria (Filkins and O'Toole 2015). *Pseudomonas* and *Burkholderia* genus, represent a main problem when colonizing these patients as their strains are highly resistant to antibiotics, and other bactericidal agents, commonly used as lung infection treatment in CF patients. The synthesis of multidrug efflux pumps, beta-lactamases and exopolysaccharides (EPS) (not only its amount, but also its composition can explain the antimicrobial resistance observed (Aaron et al. 2000; Ferreira et al. 2011). Due to that, species are able to maintain competitiveness in the environments where colonization is occurring (Bible et al. 2015). It is thought that resistance presented by these species is due to conventional biofilms (a surface attached microbial community embedded in an extracellular matrix composed by EPS and DNA) and cellular aggregates formation, a form of non-attached biofilm (Sriramulu et al. 2005). In *P. aeruginosa*, cellular aggregates are formed during the process of biofilms establishment, which formation is led by EPS production (Petrova et al. 2012) and by the repression of RetS, which usually interacts with GacS sensor protein preventing the activation of GacAS pathway and repressing biofilm formation (Goodman et al. 2009; Workentine et al. 2010). Several environmental conditions from oxidative to osmotic stress, can influence the formation of cellular aggregates. Besides environmental conditions there are some molecular players known for being responsible for cellular aggregation, such as lactate dehydrogenase. Cellular aggregation is a response to stress conditions, in which cells become more protected from external aggressions such as oxidative stress, antimicrobial therapies, and phagocytosis by the immune system. If we could prevent the formation of these aggregates, perhaps it would improve the chances of bacterial eradication by the immune system and/or antimicrobial. Due to this, the main goals of this work are: I – evaluate if cellular aggregation is conserved throughout chronic infection of CF lung by *B. multivorans*; II – Identify environmental conditions triggering aggregation; III – Confirm whether the enzyme lactate dehydrogenase is a player in this process (similarly to previous findings in another *B. multivorans* and *P. aeruginosa*); and IV – Evolve the cellular aggregation phenotype under laboratory conditions in order to find key genetic players.

Materials and Methods

Bacterial strains and growth conditions

Bacterial strains used during the studies are *Burkholderia multivorans* isolates recovered from Cystic Fibrosis patients. To test the presence of cellular aggregates, the different isolates were inoculated for 72h, at 37ºC and 180 rpm in S medium (12.5 g Na_2HPO_4, 3 g KH_2SO_4, 1 g NaCl, 1 g casaminoacids, 1 g yeast extract, 0.2 g/L Mg^{2+}, 0.001 g/L Fe^{2+} and 0.01 g/L Ca^{2+}) supplemented with 2% of Mannitol (SM medium).

B. multivorans ΔldhA mutant construction

In a first approach the two flanking regions of *ldhA* gene belonging to *B. multivorans* isolate P0213-1 were amplified by PCR. Both genes are up and downstream of the *ldhA* gene, respectively. For the amplification process, genomic DNA was extracted (QIAGEN® DNeasy® Blood and Tissue kit) and the following primers sets, including restriction enzymes, were used to each gene: *ldhR* gene; (Forward and Reverse, respectively)
5'GGGGTACCCCGGGCCAAAAATACGCAAG3'
5' GCTCTAGACGGCTGCTGAACAGGATCAC3'
Bmul_2559 gene (Forward and Reverse, respectively):
5'GCTCTAGATATCGTTCGCCGACCTTC3', and
5'GGAGCTCGCGATAGCGGCGATTCTA3'.
After being cloned into $pBCSK^+$ vector a trimethoprim resistance cassette was cloned in order to construct the final vector (pSG18-3). Triparental conjugation protocol was performed in which *B. multivorans* P0213-1 isolate was the receptor strain, in order to obtain the mutant strain. Complementation assays were performed using pARG015-1 strain (Silva et al 2017) which is a pBBR1MCS derivative containing a *HindIII* fragment expressing *LdhRA* from their own promoters.

Exopolysaccharide quantification

The amount of exopolysaccharide produced was measured based on the dry weight of the ethanol-precipitated polysaccharide recovered from 50 mL cultures grown in EPS-producing medium (SM medium) for 2 days at 37°C with agitation at 250 rpm (Silva et.al).

Biofilms formation

Biofilms were performed following the protocol described by (Ferreira et al. 2007) followed by a NaCl washing step and solubilization with ethanol.

Microscopy Observation

To analyse the phonotypic changes after the stressful growth and, to understand which strains from each isolate were, or not, capable of producing cellular aggregates, microscopic observations were performed. Once cellular aggregates present large dimensions, low objectives were used (10x, from Zeiss Axioplan microscope). Photographs were taken in order to document all images that were visualized through Axiocam 503 color Zeiss camera adapted to the microscope. The program used to visualize the live images from the microscope and capture them was ZEN software.

Estimation of biomass in aggregates or as free cells by dry weight

After the visualization of the phenotypic variations, quantification of the amount of aggregated and non-aggregated cells was performed. For this, a specific protocol was developed based on the protocol described by Haaber *et.al*. After incubation, in the previously described conditions, the growth cultures were transferred to 50 mL tubes and centrifuged at 1400 rpm at 20ºC for 30 seconds. After centrifugation, the suspensions rested for 10 minutes, without any movement, so the aggregates that were still in suspension could settle in the pellet. Then, the supernatant was removed by pipetting and placed in new 50 mL tubes, corresponding to the non-aggregated cells, that were centrifuged for at least ten minutes at 4000 rpm, so the non-aggregated cells could be separated from the growth medium. The resulting pellet was resuspended in the remaining five millilitre growth medium, and then several centrifugations, at 13200 rpm for two minutes, were performed in 2 mL eppendorf tubes in order to collect all cells from the same stress in the same tube. The suspensions containing the aggregates were also moved to 2 mL eppendorf tubes. After all the centrifugations, the 2 mL eppendorfs are opened and stay at 60ºC until all the aggregates and non-aggregated cells are completely dried, presenting a brown colour. This process usually takes 72h, depending on the density of the presenting sample. Before the samples are placed into the eppendorfs, the tubes are weighted; the same procedure is performed after the samples are dried after the 72h at 60ºC.

Laboratory evolution experiment with isolate *B. multivorans* P0426-3

Isolate P0426-3 was inoculated in SM medium for 30 days, at 37ºC and 180 rpm. Every two/three days 1 ml of the inoculum was re-inoculated in new SM medium. After the 30 days 1 ml of the inoculum was serially diluted and plated onto solid LB medium. Different colonies were selected and inoculated in liquid LB medium and preserved in 30% glycerol at -80ºC.
Genomic DNA of *B. multivorans* P0426-3T30 mutant was extracted using QIAGEN® DNeasy® Blood and Tissue kit. The DNA sample was processed according to Illumina's instructions for generating paired-end libraries, which were sequenced using Illumina Nextseq system at Instituto Gulbenkian de Ciência (Portugal). To polish and filter reads, Sickle Filter reads software was used, followed by reference assembly. In this

strategy the evolved P0426-3T30 reads were assembled against a previously sequenced P0426-3 isolate genome. To align the reads BWA v0.7.15 was used. After the alignment, gene prediction and annotation were performed with Prokka (Seemann 2014) program. A visual inspection of the alignments using Geneious v.6.1.8 (Kearse et al. 2012) allowed the confirmation of each indel and SNP mutations.

Results and Discussion

Intrinsic ability of *B. multivorans* clinical isolates to form cellular aggregates

The first aim of this study was to evaluate cellular aggregates formation by longitudinal series of *B. multivorans* recovered from cystic fibrosis patient's lung infections. Together, 129 isolates of *B. multivorans* (120) and *B. pseudomultivorans* (9) recovered from 9 CF patients were tested. The standard growth conditions included incubating cells in SM medium for 72h at 37ºC with 180 rpm of orbital agitation. Following this period, cultures were analysed macroscopically and microscopically for the presence and size of planktonic cellular aggregates.

From patient P0213 were recovered 16 isolates in the period of 1996-2010. Macroscopic analysis of the 72 hours culture medium revealed the presence of many aggregates of sizes that can go up to 5 mm, in all isolates except P0213-13. This last isolate still produced aggregates, but very few in number and with a smaller size. Microscopic analysis of these aggregates showed highly branched structures resembling the root system of some plants (Data not shown). Despite some variation in this root-like structure among the different isolates, P0213-13 aggregates are more compact and not showing the branching pattern. From this analysis we conclude that the cellular aggregation trait was conserved during this chronic infection.

During the period of 2004-2012 were recovered 10 isolates from patient P0342. Macroscopic analysis of the culture medium indicated that only isolates P0342-9 and P0342-10 were able to form visible aggregates. Nevertheless, when these cultures were visualized at the microscope (Data not shown), all except P0342-2 and P0342-3 were able to form aggregates. The estimated size of aggregates from P0342-1 and P0342-4 ranged from 37-46 µm, while from P0342-5, -6, -7 and -8 were smaller. These isolates have irregular shapes. In this patient, most of the isolates are able to form aggregates, and in the two last ones, this ability was even increased.

From patient P0148 it was recovered 11 isolates of *B. multivorans* in a seven years period (1989-1996). Analysis of the growth medium after 72 hours incubation allowed the visualization of macroscopic cellular aggregates in all isolates. Microscopic analysis revealed that isolates P0148-1, -2, -3, -6, and -8 produced aggregates of smaller size when compared with the remaining isolates (Data not shown). In general, these aggregates have irregular shapes with small ramifications. Isolate P0148-5 aggregates shows a slightly different structure with a more compact appearance and wider ramifications arising from the aggregate. Again, this trait was conserved in all isolates recovered from this long-term colonization of CF patient lungs.

From patient P0205 were recovered 23 isolates spanning a period of 22 years (1993-2015). Analysis of the growth medium after 72 hours did not reveal the presence of macroscopic aggregates. Nevertheless, when these cultures were visualized under the microscope (Data not shown), we found a group of strains where aggregates were indeed absent (P0205-7, -10, -13, -14, -16, -19, -20, 21, -22, -23). The remaining isolates produce smaller aggregates with sizes up to 150 µm and irregular shapes. In this longitudinal series, cellular aggregates trait seems to be lost in the later isolates, at least under the tested conditions.

The 13 isolates from patient P0431 were recovered from the period between 1995-2008. Analysis of growth culture revealed the presence of macroscopic aggregates only in the first isolate, P0431-1. Nevertheless, microscopy images showed that isolates P0431-2, -3, -5, -7, and -9 also showed aggregates of small size (Data not shown). Cells from isolates P0431-10, -11, -12 and -13 seem to aggregate without producing stable structures.

Patient P0280 longitudinal series comprises 18 isolates recovered between 1995-2008. After 72 hours, growth medium showed that isolates P0280-1, -3, -6, -9, -11 and -12 are the only ones producing large cellular aggregates with sizes ranging 1- and 5-mm. Microscopic analysis (Data not shown) confirmed the presence of these aggregates, but also revealed the presence of smaller aggregates (≈ 20 µm) in isolates P0280-2, -8, -10, -13, and -14. Isolates P0280-4, 5, -7, -15, -16, -17, and -18 did not form aggregates under the tested conditions. Similarly, to the previous longitudinal series, this trait was conserved during chronic infection, but was absent in the later isolates.

From the respiratory chronic infection of patient P0339 were recovered 6 isolates in an eight-year period (1995-2003). From these six isolates none produced macroscopic aggregates. Still, the microscopic analysis (Data not shown) confirms the absence of aggregates in isolates P0339-3, -5 and -6, but its presence in P0339-1, -2, and -4. These isolates are of irregular structure, but the size of the first two isolates aggregates is larger than the ones produced by P0339-4 isolate.

The longitudinal series recovered between 1997 and 2014 from P0426 patient comprises 21 isolates. Macroscopic aggregates were only visualized in the cultures of P0426-1, -12, and -16. When the different growth cultures were analysed at the microscope two additional isolates had smaller aggregates, namely P0426-9 and P0426-17. The remaining isolates did not allow aggregates visualization (Data not shown). During the chronic lung infection of this patient,

this trait was not conserved, being present in a minority of the isolates.
The longitudinal series of patient P0686 comprises 11 isolates. Isolates P0686-2 and P0686-3 are *B. multivorans* while the remaining isolates are *B. pseudomultivorans*. From all isolates only P0686-10 produced macroscopic aggregates. The microscopic analysis showed small aggregates in *B. multivorans* isolates, but except for P0686-10 isolate, none of the *B. pseudomultivorans* displayed this ability.

Results of this systematic analysis of aggregates formation ability in *Burkholderia multivorans* (and small set of B. *pseudomultivorans*) is resumed in Figure 1. This figure shows that the majority of the isolates form cellular aggregates when grown in a medium with high C/N ratio; this trait is conserved during long periods of respiratory infection and, when lost, it happened more frequently in late isolates.

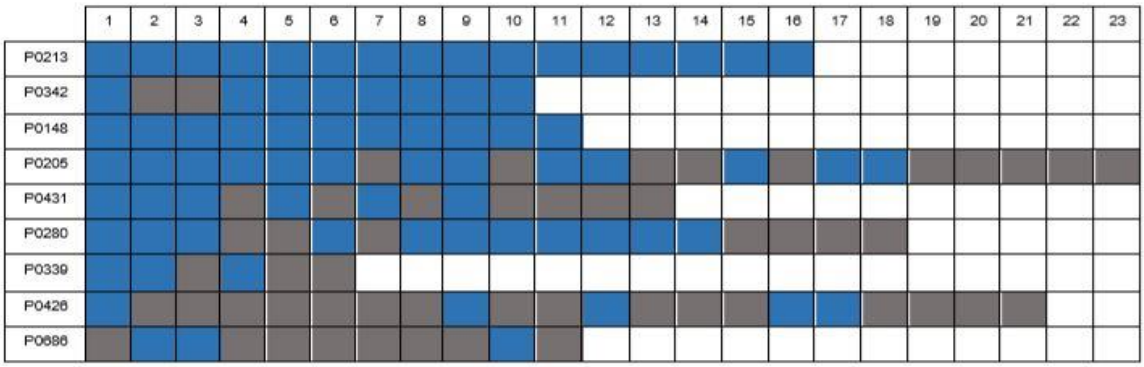

Figure 1 Schematic representation of isolates ability to produce cellular aggregates in SM medium. Blue squares represent the ability to produce cellular aggregates, whereas grey squares represent the inability to produce such structures

Environmental conditions triggering aggregates formation

After having demonstrated the ability of clinical isolates of *B. multivorans* to form cellular aggregates in SM medium, it is our aim to investigate whether this trait changes with different media or under different stress conditions. To do that, there is the need to develop an experimental procedure for quantification of cellular aggregates. One possibility was to use a sieve that retains aggregates, but it turned out to be impossible to remove aggregates from the sieve. Also, it would not retain smaller aggregates. Therefore, it was tested a different method which includes centrifugation at low centrifugation force to pellet aggregates, removal of the free cells to a new tube, followed by centrifugation at high centrifugation force; dry both cellular pellets at 60ºC; and weight them. The percentage of aggregates refers to the total weight of cells.

Influence of growth medium in cellular aggregates formation

Due to the high number of clinical isolates that we have analysed, it would be impractical to continue with all of them. Therefore, the following experiment only include isolates P0213-1, P0342-1, P0342-2, P0342-3, P0148-1, P0148-3, P0148-6, P0205-1, P0205-7, and P0205-10. From this list, P0342-2, P0342-3, P0205-7 and P0205-10 were unable to form cellular aggregates in SM medium as previously shown by the microscopic analysis,

Quantification of aggregates from the referred isolates grown in SM medium at 37ºC, 180 rpm for 48 hours shows that in P0213-1 isolate, 61.6% of the cells are present as aggregates (Figure 2), confirming the high ability to form this type of structures. In the other isolates, which do form aggregates in SM medium (P0342-1, P0148-1, P0148-3, P0148-6 and P0205-1), this value is below 8%. The remaining isolates (P0342-2, P0342-3, P0205-7 and P0205-10) show values below 1%, which we will consider a value of no aggregation. Since this quantification method nicely reproduced the macroscopic and microscopic evaluation previously done, we consider it appropriate for the remaining studies.

SM medium is a salts medium with high ratio of C/N and, might be stressful for cells when nitrogen sources became limited. Therefore, we tested whether a more equilibrated and richer medium such as LB would have a negative impact in cellular aggregation. Data shown in Figure 2 A confirmed the reduction of cells in the form of aggregates for P0213-1, all P0148 isolates, and P0205-1, but not for P0342-1 isolate. Isolates P0205-7 and P0205-10, which were unable to aggregate in SM medium, are also unable to aggregate in LB medium. Against this trend are the isolates P0342-2 and P0342-3 which are producing aggregates in LB but not in SM. Images of the aggregates formed by P0342 isolates are shown in Figure 2 B. Overall, we can

conclude that growth in LB medium leads to lower aggregation of cells, but there are exceptions.

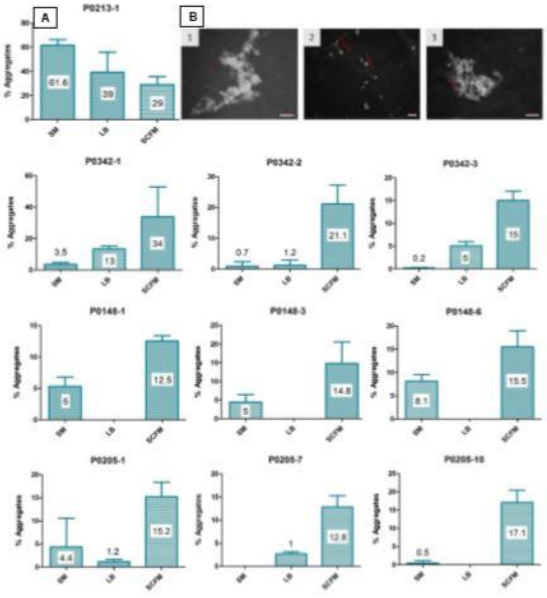

Figure 2 A – Percentage of cells in the form of aggregates as estimated by dry weight in the chosen isolates from the 9 patients after growing in different growth medium. Error bars correspond to the standard deviation of the means of at least 3 different replicas; B - Cellular aggregates of patient P0342 isolates after growth in LB medium. Images have a magnification of 100x and were obtained with ZEN software. White bars correspond to the used scale for cellular aggregates measurement (100 µm).

Because SM and LB media do not mimic the lung environment, we decided to use synthetic cystic fibrosis medium (SCFM) developed by Palmer et al (2007). Besides salts, this medium contains all amino acids and, is thought to be closer to the CF lung environment. Isolates under study were grown for 48 hours at 37ºC, 180 rpm. Results indicate that all of them are able to form aggregates in this medium, and except for P0213-1, the percentage of aggregates increased considerably (Figure 2 A). Microscopic analysis (Data not shown) of the 48 hours growth cultures show that P0213-1 isolate still forms macroscopic aggregates with many ramifications, but with a structure less compact than in SM medium, that P0342 isolates have aggregate sizes between a few micrometres up to 100 µm, that P0148 isolates have differences in the sizes of the aggregates, with P0148-1 aggregates being smaller (below 50 µm) than the two other isolates which can go to 450 µm in P0148-3 and 160 µm in P0148-6 and, that from the last studied group isolates P0205-7 and P0205-10 produce aggregates no bigger than 100 µm, while in P0205-1, these aggregates are even smaller.

With this set of experiments here described, we can conclude that the composition of the growth medium is determinant for the outcome of cellular aggregation. LB medium, being perhaps more balanced, leads to a lower number of strains being able to aggregate. SM medium induced the formation of aggregates possibly due to nitrogen limitation. In *Azospirillum brasilense* it has been reported that nitrogen limitation triggers cellular aggregation (Bible et al. 2015), suggesting that this might be the reason for increased *B. multivorans* aggregation. The last tested medium, SCFM, was the one with stronger impact in the number of isolates being able to form aggregates. A previous study where *Pseudomonas aeruginosa* was grown in artificial sputum medium rich in amino acids showed the ability of these microorganisms to form microcolonies (Sriramulu et al. 2005). Contrastingly, in a medium without amino acids, no microcolonies were observed, leading to the hypothesis that amino acids might be the cause for this difference. It would perhaps be interesting to deplete the SCFM with one amino acid at a time to see whether some amino acid(s) is relevant.

Stress conditions triggering cellular aggregates formation

The aim of this section is to evaluate if different stresses affect cellular aggregates formation. The chosen stresses are: sub-inhibitory concentration of ciprofloxacin, excess of nitrogen source, Mg^{2+} limitation, oxidative stress caused by H_2O_2 and osmotic stress.

Ciprofloxacin is a second-generation quinolone inhibiting DNA topoisomerases and DNA gyrase and, is frequently administered to CF patients with respiratory infections. Therefore, it was considered an interesting antimicrobial for the purpose of this work. Because the aim of this work was not to kill the cell culture, a sub-inhibitory concentration of ciprofloxacin was chosen to perform the study.

Each culture was then incubated in SM medium supplemented with the sub-inhibitory concentration of ciprofloxacin at 37ºC for 48 hours and 180 rpm. The percentage of cells found as aggregates was determined and results are shown in Figure 3. When compared with SM medium only, all isolates except P0213-1 showed increased percentage of biomass in the form of aggregates. This is also true for isolates P0342-2, P0342-3, P0205-7 and P0205-10 which did not form aggregates in SM but can do it in the presence of ciprofloxacin.

The presence of ciprofloxacin leads to an increase of DNA scission rates and inhibition of the ability of topoisomerase to re-ligate cleaved DNA (Anderson et al 1998), which will decrease cell replication and transcription (Hangas et al. 2018). To combat the negative effects of the antibiotic, cells in the proximity will aggregate. Inside these aggregates, concentration gradients are established (Zhang et al. 2011), promoting resistance against stressful environments. It is possible that by creating a gradient in the

aggregate, cells would be protected from the negative effects of the antibiotic.

all, most likely the opposite. If this has to be included on the list of possible stressors affecting

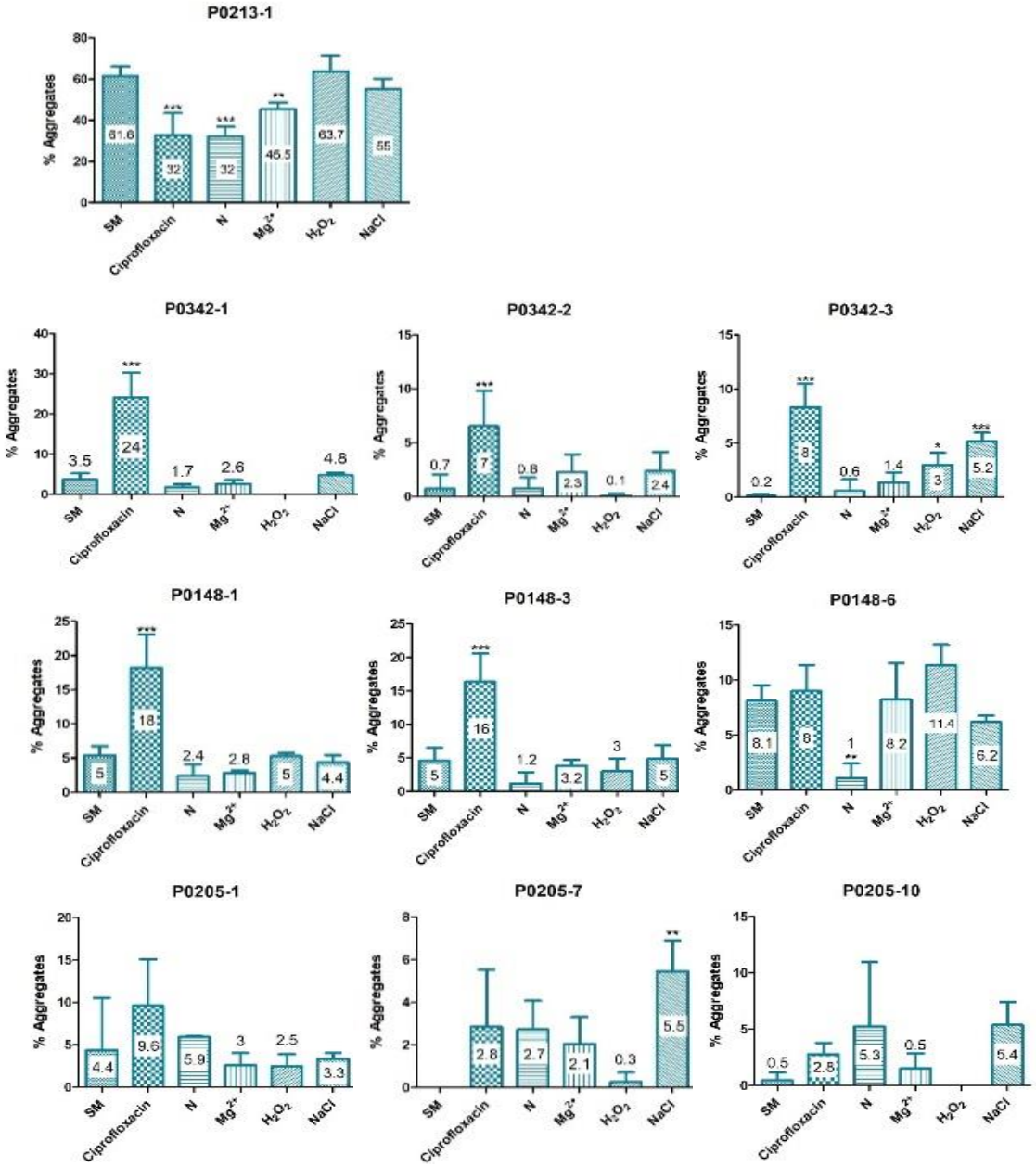

Figure 3 Percentage of cells in the form of aggregates as estimated by dry weight in the chosen isolates belonging to the 9 different patients after a 48h growth in the several stress conditions. Error bars correspond to standard deviation of the means of at least three different replicas. Statistical analysis between stress and control conditions was performed using one-way ANOVA Dunnett's test. Only results with statistical significance P-value<0.05 were considered significant. (*, *P*-value<0.05; **, *P*-value<0.01; ***, *P*-value<0.001).

Since in *Azospirillum brasilense* high concentration of nitrogen was also stressful for cells (Bible et al. 2015), we tested whether increasing casaminoacids from 1g/L to 5g/L would benefit cellular aggregation. The results obtained differed significantly between isolates. While for P0213-1 and all P0148 isolates we observed a negative effect on aggregation, in P0342 isolates there was no difference between the two conditions (Figure 3). The positive effect on aggregation was only visible for P0205 isolates, but the huge error bars prevent solid conclusions. The most likely explanation is that the amount of casaminoacids was not stressful al cellular aggregates formation, then higher concentration has to be used.

Magnesium is an important activator of cellular enzymes involved in several metabolic pathways, such as the glycolytic and glyoxylate pathways (Cowan 2002). To study the effect of magnesium limitation in cellular aggregates formation, the Mg^{2+} concentration in SM medium was reduced from 8 to 0.02 mM. Data from Figure 3 shows a general negative effect on aggregation. Microscopic images confirm that isolates that do not form aggregates in SM also do not form in SM medium depleted from Mg^{2+}. Overall, under the tested conditions, magnesium limitation did not

trigger cellular aggregation, but perhaps we are not under limiting conditions since other components of SM medium might have traces of this ion.

Another stress under study was oxidative stress generated by hydrogen peroxide. Since *Burkholderia* is known to be highly sensitive to this compound, a very low concentration (0.005 % (v/v)) was used. As shown in Figure 3, there are no significant differences between SM and SM supplemented with H_2O_2, perhaps with the exception of P0342-3 which did not produce detectable aggregates in SM but does it in the presence of H_2O_2. In this experiment, it was observed some growth arrest in the first hours and only then growth resumed. Perhaps lower concentrations of H_2O_2 should be tested.

The last stress condition imposed to the isolates under study was osmotic stress. For that, instead of normal 1g/L of NaCl in SM medium, we added 10 g/L. The effect in cellular aggregation was strain specific. No significant differences were observed for P0213-1 and for P0148 isolates, while P0342 and P0205 isolates increased the amount of biomass in the form of aggregates (Figure 3).

In a previous study on the response to osmotic stress by *Burkholderia*, Behrends et al (2011) concluded that each strain responds differently. In their study, they demonstrated that several metabolites such as alanine, phenylalanine, glutamate, trehalose and glycine-betaine can be produced and grouped as osmotic tolerance strategies into three categories: I – isolates that induce metabolic changes in response to osmotic stress by increasing the levels of all osmo-responsive compounds; II – isolates where only amino acids increase their levels, but the production of glycinebetaine and trehalose is null; and III – isolates where only glycine-betaine levels increase. It is then possible to conclude that each strain may respond differently to this stress and that also impacts differently their aggregation phenotype.

Taken together, our results show that sub-inhibitory concentration of ciprofloxacin is the best trigger of cellular aggregates formation. Other stresses such as oxidative and osmotic stresses might also have an impact, but it seems to be more strain-specific.

Deletion of *ldhA* gene from *B. multivorans* P0213-1 genome and its impact on aggregates formation

To evaluate whether D-lactate dehydrogenase LdhA from P0213-1 also plays a role in cellular aggregation, wild-type and mutant were incubated in SM medium and grown for 48 hours at 37ºC, 180 rpm. Macroscopic analysis of the two cultures showed lower number of aggregates in the *ΔldhA* mutant, which also presented smaller size. Microscopic analysis of the aggregates showed the same type of root-like structure already described (Figure 4) Size estimation of the several isolates indicated values over 1000 µm for the wild-type while the mutant aggregates had less than 600 µm.

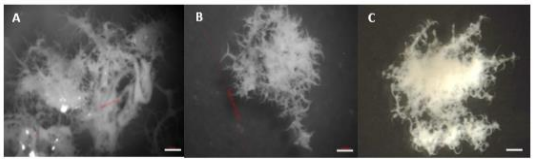

Figure 4 Cellular aggregates produced by P0213-1 (A - wild-type), *ΔldhA* (B - mutant) and complemented mutant (C complemented) when grown in S medium with 2% D-mannitol for 48h at 37ºC and 180 rpm. The three images were obtained by magnifier observation using ZEN software. (A) – Image have a magnification of 32x, and the presented aggregate has a size of 1105.355 µm; (B) – Image have a magnification of 25x, and the cellular aggregate presented has a size of 1073.125 µm; (C) – Image have a magnification of 20x. White bars correspond to the used scale for cellular aggregates measurement (100 µm).

Quantification of aggregates and free cells confirm a reduction of biomass present in the form of aggregates by the *ΔldhA* mutant. Overexpression of LdhA in the mutant strongly increased the amount of aggregates, with the value reaching approximately 97% while the mutant showed 46% and the wild-type 62%, as determined from the dry weight of biomass (Figure 5 A).

As previously said, in *P. aeruginosa* the two-component regulator MifR is responsible for micocolonies formation (Petrova et al. 2012). However, such phenotype is also dependent of pyruvate fermentation, once the inactivation of genes encoding lactate dehydrogenase led to phenotypes similar to those observed in *mifR* mutants (lack of cellular aggregates). It is thought that within cellular aggregates cells experience oxygen-limiting and energy-rich conditions leading to pyruvate fermentation as a way of maintaining redox balancing, (Silva et al 2017; Petrova et al. 2012). According to Silva et. al (2017) the contribution of *B. multivorans* ATCC 17616 D-lactate dehydrogenase in cellular aggregates formation may be also due to the anoxic environment within the aggregates, inducing cells to ferment pyruvate (the process involves the conversion of pyruvate into lactate) as a way of redox balancing. With this, it would be expected the production of smaller cellular aggregates by *ΔldhA* mutant when comparing with the WT strain. This is in line with the present results, since the decrease of cellular aggregates production can be a consequence of the absence of pyruvate fermentation. It was also possible to conclude that LdhA activity contributes to cellular aggregates formation, however it is not the only factor contributing to this phenotype, as the mutant strain continues to produce cellular aggregates.

To evaluate whether the *ldhA* mutation also plays a role in surface attached biofilm formation, assays were conducted for the wild-type strain, *ΔldhA* mutant and complemented mutant. Crystal violet staining of biofilms showed no differences between the wild-type and mutant, but the ability of the complemented mutant to produce biofilm was significantly higher (Figure 5 B). The phenotype of the mutant contrast with the one obtained by (Silva et al 2017) for *B. multivorans*

ATCC 17616 which showed a reduction in the ability to form biofilms. Nevertheless, the fact that overexpression of *ldhA* gene increases the amount of biofilm is an indication that lactate dehydrogenase plays a role in biofilms.

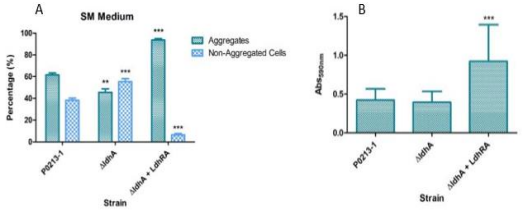

Figure 5 A - Dry weight results of P0213-1, *ΔldhA* and complemented mutant. Error bars represent the standard deviation of the means values of at least 3 replicates. **B** - Biofilm formation of P0213-1 isolate, *ΔldhA* mutant and complemented mutant, after 48h growth in polystyrene microplates at 37ºC. Error bars represent the standard deviation of the means values for at least 12 replicates Statistical significance of differences between P0213-1 and the remaining strains was determined by one-way ANOVA followed by Dunnett's multiple comparisons test. (**, *P*-value < 0.01; ***, *P*-value < 0.001).

Since mutation of *ldhR* and *ldhA* in *B. multivorans* ATCC 17616 had a positive effect in the production of exopolysaccharide, the same was evaluated for the strains under study. To do that, the wild-type, *ΔldhA* mutant and complemented mutant were grown in SM medium for 48 hours. Then, the free cells supernatant was mixed with 3 volumes of ethanol to precipitate polysaccharides. Dry-weight determination confirmed the production of exopolysaccharide in the wild-type strain (Figure 6 A), but unexpectedly no polysaccharide was precipitated from the mutant and complemented mutant. Still, when both wild-type and mutant were grown in solid YEM, both displayed similar mucoid phenotype (Figure 6 B). At the moment we have no explanation for the differences between solid and liquid media regarding exopolysaccharide production.

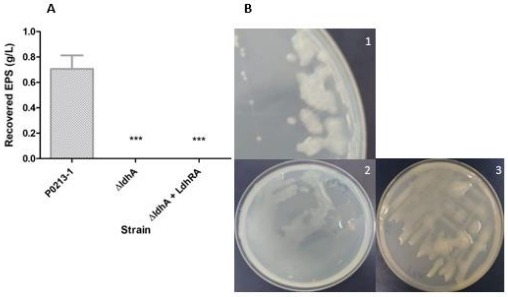

Figure 6 A- Exopolysaccharide production of wild-type P0213-1, *ΔldhA* mutant and *ΔldhA* complement, based on the dry weight of ethanol-precipitated EPS after 48h growth at 37ºC. Error bars correspond to the standard deviation of the mean values of three replicas. Statistical significance was determined by one-way ANOVA followed by Dunnett's multiple comparisons test. Differences were only considered significant for *P*-values<0.05. (***, *P*-value<0.001). **B** - Mucoid phenotype of P0213-1 (A), *ΔldhA* mutant (B) and complemented mutant (C) in yeast extract mannitol medium (YEM) after 48h incubation at 37ºC.

Evolution of the cellular aggregation trait under laboratory conditions

The aim of the following experiments was to observe if under laboratory settings free-living cells could evolve the cell aggregation phenotype, by growing them for many generations. The choice was isolate P0426-3, unable to form cell aggregates in SM medium. The experimental setting used was to grow this isolate in SM medium for 48 hours, 37ºC and 180 rpm and, then inoculate 1 ml culture into new medium for another 48 hours and so on up to 13 passages (30 days total). Before every passage, an aliquot was analysed under the microscope to search for the presence of cellular aggregates. Analysis of microscopy images showed cellular aggregation for the first time at day 7. The size and shape of the aggregates remained more or less the same in the following days, but at the end of the experiment, aggregates were bigger and more compact. At the last time point, an aliquot was serially diluted and plated onto LB agar plates to obtain isolated colonies. One colony showing distinct morphology, namely being very dry (Figure 7) was kept for confirmation of its ability to form aggregates. Figure 7 A confirms that strain named P0426-3T30 indeed produces aggregates of sizes that can go up to 40 µm.

Figure 7 Plate images of isolate P0426-3 before long-term evolution experiment (left) and after the 30 days long-term evolution experiment (right). It is possible to see that colonies from the evolved P0426-3 present a drier appearance. A – Microscopic images of P0426-3T30 strain. It has a magnification of 100x and was obtained using ZEN software. White bar corresponds to 100 µm scale.

To identify which mutations are present in this evolved mutant, we sequenced the whole genome by using Illumina technology. Since we already have the sequence of the ancestor P0426-3 (Pessoa2017), here we performed a reference assembly by alignment of P0426-3T30 reads against P0426-3 genome, using aligner BWA-mem (Li et al. 2009). From this analysis we obtained several single nucleotide variants either in gene coding regions or intergenic regions as shown in Table 1. Three of the mutations mapped to Nodes (contigs) 4, 5 and 14 and, 8 mutations are in node 7. Two of the nonsynonymous mutations are found in a homologue of Bmul_5593, encoding a hypothetical protein and, in the *amiC* gene encoding *N*-acetylmuramyl-L-alanine amidase. The synonymous mutations are in gene *nlpD2* encoding a murein hydrolase activator and, the *flp* gene encoding a Tad-like Flp pilus assembly family protein. Contrastingly to nonsynonymous mutations, synonymous (also called "silent mutations") mutations do not change the amino acid in the final protein. Nevertheless, they might influence the amount of protein being produced, either by modifying the stability of the transcript or by changing the codon usage,

affecting the tRNA used during the translation process.

Table 1 Polymorphic genes identified among *B. multivorans* P0426-3 isolate recovered after the 30 days of long-term evolution experiment (Synonymous mutation – Syn; Non-synonymous – Nonsyn).

NODE	Position	Mutation	Gene Name	Annotation	Effect in protein	Effect of mutation
4	285529	G>C	*nlpD2*	Murein hydrolase Activatior	-	Syn
5	174949	G>C	*amiC*	*N*-acetylmuramyl-L-alanine amidase	L248R	Nonsyn
7	24021	T>C	*Flp*	Tad-like Flp pilus-assembly family protein	-	Syn
7	210873	C>A	Intergenic Region		-	-
7	210895	G>T				
7	210898	G>C				
7	210905	G>C				
7	210911	C>T				
7	210916	C>A				
7	210921	C>A				
7	210923	G>A				
14	10484	G>C	Bmul_5593	Hypothetical protein	G231R	Nonsyn

AmiC (*N*-acetylmuramyl-L-alanine amidase) is a peptidoglycan hydrolase responsible for the hydrolysation of the amide bond between MurNAc and L-alanine, separating by this the glycan strand from the peptide (Vollmer et al. 2008). These enzymes are also referred as peptidoglycan amidases or amidases. *N*-Acetylmuramyl-L-Alanine amidases (MurNAc-LAAs) are bacterial members of the autolytic system. These amidases carry a signal in their *N*-termini that enables their transport across the cytoplasmic membrane (Vollmer et al. 2008). Within bacterial proteome, many different MurNAcLAAs are present. One of the identified MurNAc-LAAs is AmiC which has a periplasmic localization, becoming soluble after the cleavage of the signal peptide (Vollmer et al. 2008). Like its homologues (AmiA and AmiB), AmiC plays an important role in cleaving the septum to release the new cells after cell division. The transport of AmiC to the septal ring is performed by the Twin-arginine transport (Tat) system. This system is responsible for the translocation of folded proteins containing cofactors across the bacterial cytoplasmatic membrane (Vollmer et al. 2008). Firstly, it was thought that AmiC did not contained a cofactor. However, after amino sequence comparisons of Bacillus polymyxa bacteriophage PSA it was suggested that AmiC and its homologous are Zn^{2+} containing metalloenzymes (Korndörfer et al. 2006). Because AmiC is involved in the process of septum cleavage which allows separation of daughter cells, so it is expected that differences in its expression and function would influence the capacity of cell division. Such facts were already observed by Vollmer et al. (Vollmer et al. 2008). In their study, it was observed that the *amiC* deletion mutant cells separate poorly during cell division. Due to this, between 20 and 30% of the cell population are in a chain form, composed by three up to six unseparated cells (Vollmer et al. 2008). It was also observed that other autolysins play an important role in the development of biofilms, being required for the formation of such structures (Heilmann et al. 1997).

However, to properly function, AmiC needs to be activated. Through direct protein-protein interactions with NlpD (a murein hydrolase activator), AmiC and other amidases activity, is controlled (Peters et al. 2013), enhancing it. NlpD is a member of the LytM family proteins which contains a LytM (peptidase M23) domain. NlpD is a lipoprotein with an *N*-terminal lipid moiety which serves as a membrane anchor (Yang et al. 2018). After its synthesis in the cytoplasm, the NlpD protein is transported to the periplasm where it anchors to the outer membrane with the *N*-terminus (Yang et al. 2018). This protein physically interacts with the peptidoglycan, being this interaction specific. Although being important for the separation of daughter cells, it was observed that in *E. coli* and in *Xanthomonas campestris* NlpD does not have by itself a peptidoglycan hydrolytic activity (Yang et al. 2018). NlpD influences cell division by modulating AmiC activity to hydrolase peptidoglycan, this is, activates AmiC activity (Yang et al. 2018), being its activity indispensable to a proper cell division. Interestingly, in our evolved strain, P0426-3T30, both *nlpD* and *amiC* genes were mutated. Although, we cannot predict whether these mutations have positive or negative effects on enzyme activity, it is possible that they effect cell division, by preventing cells to separate. That way, they would stay together and form aggregates.

Beside the mutations in genes related to peptidoglycan degradation, namely in cell division, a gene related to the expression of the adhesive Flp (fimbrial low-molecular-weight protein) pili also suffered a mutation. This type of pili is synthesized by the products of *tad* genes (Tad from tight adherence). They encode a machinery known as the Tad macromolecular transport system, that is required for the assembly of the Flp pili (Tomich et al. 2007). The tad locus is composed of 14 different genes, being the first one (*flp-1* gene) the one which encodes the major structural component of Flp pili (Tomich et al. 2007). Between 12 to 13 of these genes are essential for Flp-pilus production, autoaggregation and biofilm formation (Kachlany et al. 2000; Kachlany et al. 2001). The expression of these genes, depending on the species, varies with oxygen concentrations and quorum-sensing. *P. aeruginosa* Flp pili expression might be induced in the human host, especially when quorum-sensing pathways are activated (Tomich et al. 2007). Pili derived from the Tad macromolecular transport system can be composed of two possible types of prepilins (Type IVa and Type IVb). Type IVa prepilins have short Nterminal signal sequences (5-6 amino acids) and its mature proteins have 150 amino acids, whereas Type IVb prepilins have longer signal sequences (15-30 amino acids) and also larger mature forms (190 amino acids) (Tomich et al. 2007). All genes belonging to the tad locus are necessary to pili assembly. However, the most important one is *flp-1*. P0426-3T30 mutation that

took place in this region did not changed the amino acid of the protein (synonymous). With this, it would be expected that no alterations in the protein function would happen. However, due to the stated above, the amount of protein being produced might be different. In this case, alterations in the production of pili and, as a consequence cell adhesion could be affected. Since we observed aggregates formation, it could be that these mutant cells display higher adhesion ability. Further studies need to be done to confirm or not this hypothesis.

Seven mutations were mapped into the same intergenic region. This region contains the promoter of a putative operonic structure with two genes encoding hypothetical proteins and a sodium proton antiporter. By affecting a promoter, these mutations might have strong impact on the expression of this operonic structure.

In *E. coli*, nhaP gene encodes a Na+/H+ antiporter (NhaP). Within bacterial cells this antiporter plays several important roles such as establishment of an electrochemical potential across membranes, extrusion of Na+ which is toxic to cells when present in high concentrations, regulation of intracellular pH under alkaline conditions, and at last but not least, regulation of cell volume (Utsugi et al. 1998). Alteration in the expression of such protein might have strong effects on cell physiology. However, to understand if the observed mutations influence the expression of the downstream genes more tests and analysis should be performed.

At last, a hypothetical protein suffered a non-synonymous mutation, which means that the mutation changed the respective amino acid, and as a consequence the function of the protein can be compromised. Although the gene is not yet described, according to the String software (Szklarczyk et al. 2017) it is predicted to be an UBA/THIF-type NAD/FAD binding fold. This domain is a NAD/FAD-binding fold that interferes in the activation of E1 enzyme (Ubiquitin-activating enzyme). The role of proteins with this motif in bacteria is unknown.

Together, we can conclude that our evolution experiment was successful, since by serial passages it was possible to evolve the cell aggregates phenotype. Mutations in a gene involved in the synthesis of pili and cell division might contribute to this phenotype.

Concluding remarks and future perspectives

The importance of cellular aggregation in CF pathogens is highlighted in studies showing that in the airways of CF patients these bacteria are often found in small clusters (Worlitzsch et al. 2002; Schwab et al. 2014). Also, Silva et al. (2017) has shown that environmental and clinical isolates of several Bcc species are able to form microscopic to macroscopic aggregates in vitro. Our hypothesis is that the establishment of a chronic infection requires adaptations, including cell aggregation, as a way to mitigate the stresses present in the CF lung.

This work started by analysing approximately 130 CF clinical isolates of *B. multivorans* for their ability to aggregate in SM medium. Data confirmed that the majority of the isolates do form aggregates and some who did not were late isolates within the longitudinal series. Then it was tested whether growth in a medium mimicking the nutrients found in the lungs would have an impact in cell aggregation. Interestingly, all tested isolates, even the ones unable to aggregate in SM medium, were able to form cellular aggregates. The search for environmental conditions triggering aggregates formation, revealed that sub-inhibitory concentrations of ciprofloxacin was the best trigger, increasing the biomass present as aggregates in most of the isolates. Other stresses such as hydrogen peroxide and osmotic stress had an effect, but it was isolate-specific. Together, our results confirmed an intrinsic ability of *B. multivorans* isolates to form cell aggregates and this can be enhanced by stress conditions similar to the ones found in the CF lung.

Previous studies have identified lactate dehydrogenase as important for aggregates formation both in *B. multivorans* (Silva et al 2017) and Pseudomonas aeruginosa (Petrova et al. 2012). Here, we want to evaluate whether this gene was also implicated in aggregates formation in *B. multivorans* P0213-1 clinical isolate. The *ldhA* mutant was successfully constructed, and its role in cellular aggregation confirmed. Interestingly, deletion of this gene decreased the biomass of aggregates, but its overexpression had stronger influence, with the amount of aggregates biomass increasing to more than 90%. We believed the importance of this protein might be with the fermentation of pyruvate into D-lactate within the hypoxic zones of the aggregate in order to obtain energy.

The last set of experiments performed aimed to evolve the aggregation phenotype under laboratory conditions and identify mutations that could be responsible for inducing that phenotype. By serial passages of isolate P0426-3 (which was growing as free cells) in SM medium we were able to trigger the aggregation phenotype at day 7 of the evolution experiment. Sequencing the genome of a colony obtained at day 30 allowed to identify several mutations when compared to the ancestor. These mutations mapped into genes affecting adhesion, cell division and hypothetical proteins. It is likely that some of them might be responsible for the observed phenotype.

This work gave some insights into the prevalence of the cellular aggregation trait in *B. multivorans* clinical isolates; identified some environmental triggers; confirmed the role of a metabolic enzyme in the formation of aggregates with increased size; and identified new putative genes with a role in the trait under study. Still, a lot of work has to be done, particularly by testing all *B. multivorans* clinical isolates in SCFM medium; confirming if the role of lactate dehydrogenase in cell aggregation is through energy generation or if it is mediated by lactate signalling; repeat the evolution experiment with more replicates to

identify other mutations; and analyse the role of Flp pilus in aggregates formation. Despite all we still have to discover, we believe that these multicellular structures might confer higher protection against the immune system and antimicrobial, thus enabling cells to persist.

References

Aaron, Shawn D, Wendy Ferris, Deborah A Henry, David P Speert, and Noni E M A C Donald. 2000. "Multiple Combination Bactericidal Antibiotic Testing for Patients with Cystic Fibrosis Infected with Burkholderia Cepacia." *American Journal of Respiratory and Critical Care Medicine* 161 (16): 1206–12.

Bible, Amber N., Gurusahai K. Khalsa-Moyers, Tanmoy Mukherjee, Calvin S. Green, Priyanka Mishra, Alicia Purcell, Anastasia Aksenova, Gregory B. Hurst, and Gladys Alexandre. 2015. "Metabolic Adaptations of *Azospirillum brasilense* to Oxygen Stress by Cell-Cell Clumping and Flocculation." *Applied and Environmental Microbiology* 81 (September): AEM.02782-15. doi:10.1128/AEM.02782-15.

Ferreira, Ana S., Jorge H. Leitão, Sílvia A. Sousa, Ana M. Cosme, Isabel Sá-Correia, and Leonilde M. Moreira. 2007. "Functional Analysis of *Burkholderia cepacia* Genes BceD and BceF, Encoding a Phospholyrosine Phosphatase and a Tyrosine Autokinase, Respectively: Role in Exopolysaccharide Biosynthesis and Biofilm Formation." *Applied and Environmental Microbiology* 73 (2): 524–34. doi:10.1128/AEM.01450-06.

Ferreira, Ana S, Inês N Silva, Vítor H Oliveira, Raquel Cunha, and Leonilde M Moreira. 2011. "Insights into the Role of Extracellular Polysaccharides in *Burkholderia* Adaptation to Different Environments." *Frontiers in Cellular and Infection Microbiology* 1 (December): 1–9. doi:10.3389/fcimb.2011.00016.

Filkins, Laura M., and George A. O'Toole. 2015. "Cystic Fibrosis Lung Infections: Polymicrobial, Complex, and Hard to Treat." *PLoS Pathogens* 11 (12): 1–8. doi:10.1371/journal.ppat.1005258.

Goodman, Andrew L., Massimo Merighi, Mamoru Hyodo, Isabelle Ventre, Alain Filloux, and Stephen Lory. 2009. "Direct Interaction between Sensor Kinase Proteins Mediates Acute and Chronic Disease Phenotypes in a Bacterial Pathogen." *Genes and Development* 23 (2): 249–59. doi:10.1101/gad.1739009.

Haaber, Jakob, Marianne Thorup Cohn, Dorte Frees, Thorbjørn Joest Andersen, and Hanne Ingmer. 2012. "Planktonic Aggregates of *Staphylococcus aureus* Protect against Common Antibiotics." *PLoS ONE* 7 (7): 1–12. doi:10.1371/journal.pone.0041075.

Inês N. Silva,a Marcelo J. Ramires,a Lisa A. Azevedo,a Ana R. Guerreiro,a Andreia C. Tavares,a* Jörg D. Becker,b Leonilde M. Moreiraa, c. 2017. "Regulator LdhR and D-Lactate Dehydrogenase LdhA of *Burkholderia multivorans* Play Roles in Carbon Overflow and in Planktonic Cellular Aggregate Formation." *Applied and Environmental Microbiology* 83 (19): 1–24.

Petrova, Olga E, Jill R Schurr, Michael J Schurr, and Karin Sauer. 2012. "Microcolony Formation by the Opportunistic Pathogen *Pseudomonas aeruginosa* Requires Pyruvate and Pyruvate Fermentation." *Molecular Microbiology* 86 (4): 819–35. doi:10.1111/mmi.12018.

Sriramulu, Dinesh D., Heinrich Lünsdorf, Joseph S. Lam, and Ute Römling. 2005. "Microcolony Formation: A Novel Biofilm Model of *Pseudomonas aeruginosa* for the Cystic Fibrosis Lung." *Journal of Medical Microbiology* 54 (7): 667–76. doi:10.1099/jmm.0.45969-0.

Workentine, Matthew L., Joe J. Harrison, Aalim M. Weljie, Vy A. Tran, Pernilla U. Stenroos, Valentina Tremaroli, Hans J. Vogel, Howard Ceri, and Raymond J. Turner. 2010. "Phenotypic and Metabolic Profiling of Colony Morphology Variants Evolved from *Pseudomonas fluorescens* Biofilms." *Environmental Microbiology* 12 (6): 1565–77. doi:10.1111/j.1462-2920.2010.02185.x.